

CGU HS Committee on River Ice Processes and the Environment 22nd Workshop on the Hydraulics of Ice-Covered Rivers

Canmore, Alberta, Canada, July 9-12, 2023.

Monitoring the formation and growth of lake ice under heavy snowfall

Arash Rafat and Homa Kheyrollah Pour

Remote Sensing of Environmental Change (ReSEC) Research Group, Department of Geography and Environmental Studies and Cold Regions Research Centre, Wilfrid Laurier University, Waterloo, ON N2L 3C5 arafat@wlu.ca, hpour@wlu.ca

Freshwater ice in the Northwest Territories, Canada serves as vital transportation infrastructure for local communities in winter. Lake ice in the Yellowknife region is heavily relied for transportation via ice roads, crossings, and winter trails- many of which traverse small lakes. However, there is currently a lack of in-situ data on the evolution of lake ice in the region, particularly during freeze-up/break-up periods when ice has a low bearing capacity. To address this knowledge gap, this study aimed to design, construct, and deploy a floating research station equipped with an automated ice sensor in a small subarctic lake, located ~12 km north of Yellowknife within the Baker Creek Research Watershed. The study was conducted between October-December 2022. Results show that freeze-up and sequent ice growth were uncharacteristically driven by snow-ice production, in contrast to thermal ice growth, because of extreme snowfall in October and November 2022. The evolution of the ice cover between October-December 2022 is framed in the context of a case study for comparing ice formation and growth during a year of significant snowfall to ice growth in a low snowfall year (November-December 2021). Findings provide insight into potential new regimes and evolutions of ice under shifting snowfall patterns in Yellowknife.

1. Introduction

Small lakes (<10 km²) are ubiquitous features of the landscape surrounding Yellowknife, Northwest Territories (NWT). These lakes typically freeze in late October/early November and commonly form a solid, primary ice cover of columnar grained, congelation ice known as black ice. The formation of the primary ice cover on these lakes is typically fast. However, besides testimonial accounts of ice formation in the region, limited efforts have been made to observe this process and subsequent growth of ice. This is notwithstanding the heavy community reliance on small lakes for winter transportation via ice roads, winter snowmachine trails, and recreation. The lack of in-situ observations of these processes is likely due to the rapid nature of the formation of the ice cover, and inadequate bearing capacity of the thin ice (e.g., <10 cm) required to obtain measurements.

Past research on ice formation and thin ice growth processes on small lakes is limited. Many of these studies have relied on modelling efforts to simulate the timing of freeze-up and subsequent evolution of the ice cover (e.gs. Duguay et al., 2003; Kheyrollah Pour et al., 2012, 2017; Launiainen & Cheng, 1998; MacKay, 2012; Yang et al., 2012). While lake ice models have great utility in the absence of field observations, they often oversimply or inaccurately parameterize ice freeze-up/break-up processes. Consequently, these models may lead to potentially inaccurate estimates of ice thicknesses or snow depths, particularly during the early ice cover season when ice thickness estimates are crucial for community safety.

In an initial attempt to monitor ice formation and thin ice growth in the region, we have designed, constructed, and deployed a floating research station in a small subarctic lake in October 2022. The floating research station houses an automated ice sensor called a Snow and Ice Mass Balance Apparatus (SIMBA), as well as a series of instrumentation beneath and adjacent to the station to monitor local environmental and meteorological parameters. Using this station, the primary objective of this study was to investigate lake ice formation and thin ice growth.

During October and November 2022, Yellowknife received ~87% and 60% more snowfall relative to the 1981-2010 climate normal (187% and 160% of normal). The magnitude and timing of this snowfall resulted in complex processes of early season ice formation and growth led by slush and snow-ice production. Using temperature data collected every 15 minutes from the floating research station, the secondary objective of this study was to investigate these complex processes between October 5- December 31st, 2022, in the context of a year with heavy snowfall. As a case study, the evolution of the ice cover during this heavy snowfall year is contrasted with ice growth between November-December 2021, which experienced 62% and 31% lower snowfall compared to the November-December 1981-2010 climate normal (38% and 69% of normal, respectively). With climate change causing increases in autumnal precipitation in the region (Spence et al., 2011), this study provides a glimpse of potential future ice growth scenarios should snowfall continually increase in Yellowknife with this changing climate.

1.1 Site Description

This study aims to investigate the formation and growth of ice within Landing Lake, a small subarctic lake ~12 km north of Yellowknife, Northwest Territories, Canada. Landing Lake has a surface area of 1.07 km² and is part of the Baker Creek Research Watershed (BCRW), about 7 km north of Yellowknife, Northwest Territories, Canada (Figure 1). The lake is morphometrically

complex, and has mean and maximum depths of 1.77 m and 4.28 m respectively (Rafat et al., 2023). Landing Lake drains a relatively large catchment of 135 km² comprising about 85% of the total watershed area of the BCRW (Spence & Hedstrom, 2018).

The BCRW is a small (155 km²) Canadian Shield subarctic watershed consisting of 349 small lakes, with mean and median surface areas of 54,000 (0.052 km²) and 88,800 m² (0.088 km²) respectively (Spence & Hedstrom, 2018). These lakes are interconnected through short channels with highly variability connectivity (Spence et al., 2010). The watershed is drained by Baker Creek which flows into Great Slave Lake. A Water Survey of Canada hydrometric gauge (07SB013) is located at the outlet of Lower Martin Lake, ~5 km south of Landing Lake. The basin is located within a region of discontinuous permafrost, with frequent transitions from permafrost to non-permafrost conditions associated with large changes in topography, vegetations, snow accumulation, hydrology and surficial geology (Morse & Wolfe, 2017; Phillips et al., 2011). Land coverage in the BCRW is split between exposed bedrock (~40%), water (~22.6%), forested hillslopes (~21.5%), and wetlands/peatlands (~15.9%). The hydrological regime in the BCRW can be best described as subarctic nival (Spence & Hedstrom, 2018).

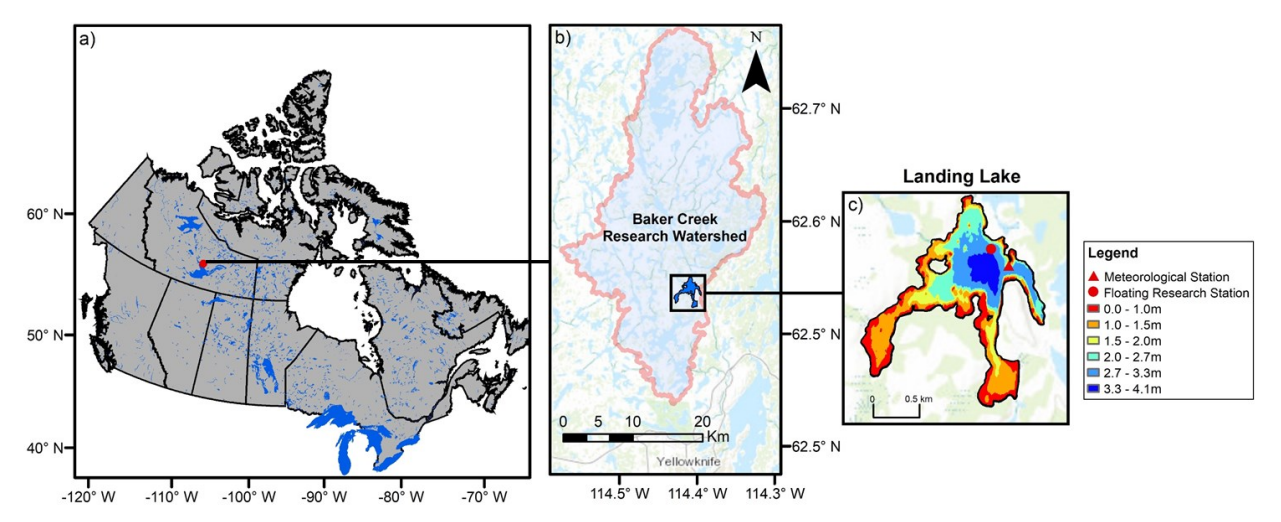


Figure 1. a) Reference map: location of Baker Creek Research Watershed (BCRW) within Canada. b) Delineation of the BCRW and Landing Lake. c) Bathymetry of Landing Lake including the locations of the floating research station and meteorological station.

2. Methodology

2.1. Floating Research Station and Meteorological Station

A floating research station was built and deployed in Landing Lake on October 5th, 2022, at a location 3.00 m deep (62.5628 N, 114.4047 W) (Figure 2a, b). The station was anchored ~250 m from an existing meteorological station operated by Environment and Climate Change Canada (Figure 2c). The meteorological station monitors all energy balance components, including turbulent fluxes estimated through the eddy covariance method. For a detailed description of instrumentation used on the meteorological station, the reader is directed to Spence and Hedstrom (2018).

The floating research station was constructed on a raft with a square 2.44 x 2.44 m (8 x 8 ft) base built using pressure treated lumber on floats (Figure 2a). A SIMBA was installed on the raft. The SIMBA consisted of a 2.9 m thermistor chain with 145 temperature sensors spaced vertically at 2 cm. Temperature profiles through air, snow, ice, and water were taken every 15 minutes. The chain was deployed 1.3 m away from the edge of the raft to minimize structural interference between the raft and the ice/snow. In addition, a small structure was deployed beneath the raft on the lakebed to measure water temperatures immediately above the sediments in the lake and water levels using a pressure transducer (Figure 2a). Water temperatures on this structure were recorded every 5 minutes using four (4) HOBO TidbiT MX400, while water levels were derived from a HOBO u20 pressure transducer on an hourly basis. Two vertical wooden planks were attached to the raft and extended into the water. One plank housed 6 additional HOBO TidbiT MX400 sensors for monitoring water (and ice) temperatures at a 5-minute frequency. The other plank housed 2 photosynthetically active radiation (PAR) loggers, for monitoring penetrating PAR into the water and beneath the ice. Under-ice (water) PAR was logged at a 15-minute frequency.

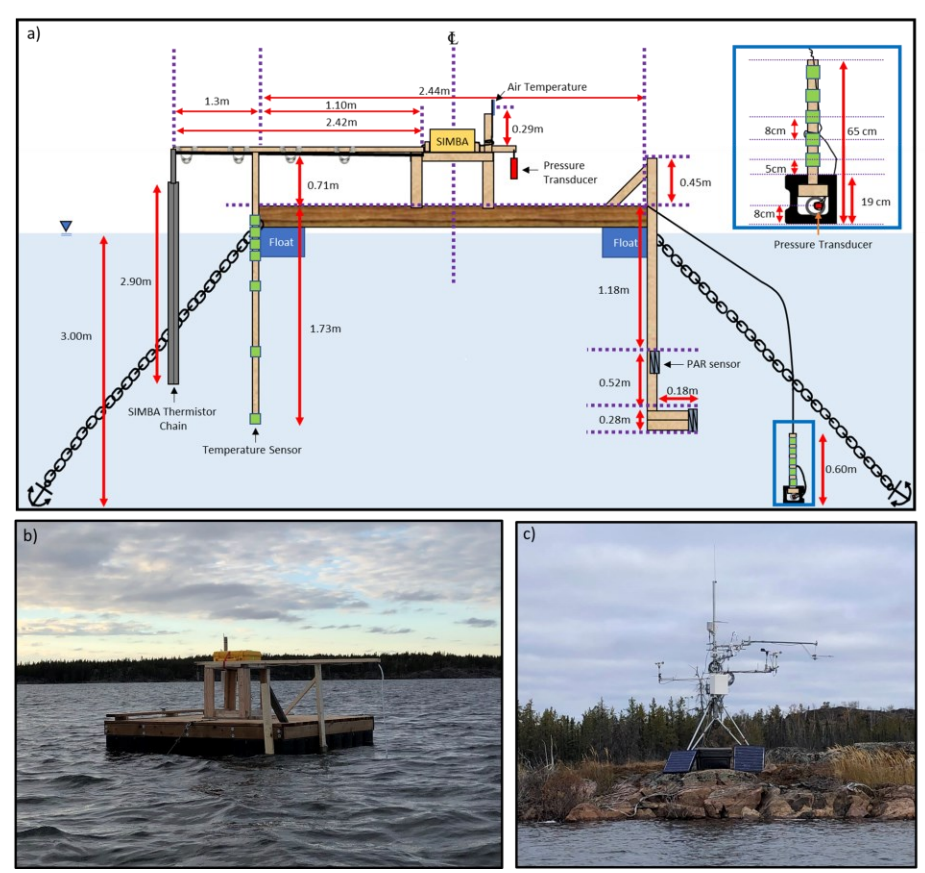


Figure 2. a) Detailed design of the floating research station, b) Operation of floating research station during the open water period. c) Meteorological station on Landing Lake operated by Environment and Climate Change

2.2. Air, snow, ice, and water interface detection

Air, snow, ice, and water interfaces were identified using the SIMBA. The SIMBA operated in two modes. Mode I took direct measurements of the ambient temperatures surrounding each sensor within the 2.9 m thermistor chain every 15 minutes. Mode II operated every 6 hours. Over a 2-

minute heating cycle, Mode II applied a 64mW constant and linear heat source to resistors housed beside each of the 145 sensors. The associated temperature rise at each resistor was recorded by adjacent temperature sensors every 30 seconds. Four (4) additional measurements are taken in the proceeding 2 minutes to measure the 'cooling' response at each resistor as the applied power is stopped. Mode II provided a means of roughly approximating the thermal conductivity ice and snow, mimicking the transient hot-wire method for measuring thermal conductivity (Healy et al., 1976; ASTM D5334) and allowed for improved interface detection (Jackson et al., 2013). However, this study does not present the thermal conductivity estimates. The SIMBA has been widely used in monitoring sea ice (e.gs. Koo et al., 2021; Lei et al., 2018), and more recently in river ice (Lynch et al., 2021), and lake ice evolution (Cheng et al., 2021; Rafat et al., 2023).

The position of the ice (or water) surface was identified by combining the information from Mode I and Mode II of the SIMBA. The temperature rise after 2 minutes of gentle heating was lower in water compared to air, as water has a larger heat capacity. Likewise, the temperature rise in ice was lower as compared to air, given ice's comparably large thermal conductivity and density, thereby effectively transferring heat away from the source. As compared to one another however, the temperature rise in water, ice, and slush are relatively similar, normally ranging between 0.4°C and 0.75° C. Snow is excluded from this range as temperature rises in snow are significantly higher. Therefore, beginning at the top of the chain, the position of either the water, ice, or slush surface would be the first sensor where the temperature rise after 2 minutes of heating would be between 0.4° C and 0.75° C. To delineate between water and ice, Mode I measurements at the identified location were analyzed. If the temperature (T) at this location was $\leq -0.5^{\circ}$ C, the surface was identified as ice, if $T \geq 0.125^{\circ}$ C the surface was water, and if -0.5° C $< T < 0.125^{\circ}$ C, the surface was likely unfrozen slush.

The position of the air-snow interface was identified by selecting the location where the spatial derivative was a maximum, beginning from the top of the thermistor chain. Since snow is an effective insulator, vertical gradients in temperatures would present a distinct peak when transitioning from air to snow. To identify the position of the ice bottom, Mode I of the SIMBA was used. For each measurement, the thermistor chain was searched between the bottom of the chain and the identified ice (or water) surface. The first sensor with a temperature (T) between - 0.5°C < T < -0.0625°C was selected to be position of the ice bottom, provided that the sensor immediately above this identified location also fell within the noted range to reduce uncertainty. The range was selected to account for manufacturer reported accuracies of the sensors and the minimum resolution of the thermistors of ± 0.0625 °C. Further details on interface detection and its validation in Landing Lake is presented in Rafat et al. (2023).

3. Results

3.1. Extreme October and November Snowfall in Yellowknife

Total snowfall data for the 2022-2023 ice cover season (October 2022- May 2023) was recorded at the Yellowknife Airport Meteorological Station, ~10 km south of Landing Lake. The first snowfall of the season was recorded on October 11th, 2023, at 3pm MST. Between October 11th - 31st, ~40 cm of snowfall occurred, amounting to 222% and 187% the mean October snowfall of the preceding 30-year record (1992-2021) and climate normal period (1981-2010), respectively (Figure 3a). A similar pattern of increased snowfall was observed in November 2022, with 176%

and 160% the preceding 30-year record and the climate normal snowfalls, respectively. The relatively extreme snowfall events followed a period of unusual low snowfall in the year previous between September-December 2021.

To determine the presence of a long-term trend in monthly snowfall totals over the available record (1942-2022), a Mann-Kendall analysis was conducted. Results indicated that there was no significant trend in September, October, and December snowfall totals at a 5% significance level, failing to reject the null hypothesis. However, snowfall totals in November showed a significant increasing trend between 1942-2022 (p=0.01, α =0.05), particularly during the early record (1942-1960) (Figure 3b). Sen's slope estimator was calculated to be 0.18 cm yr⁻¹ for November snowfall. Total snowfall recorded between September to December over the 1942-2022 record showed an increasing trend (p=0.02, α =0.05) of 0.32 cm yr⁻¹ (Figure 3c).

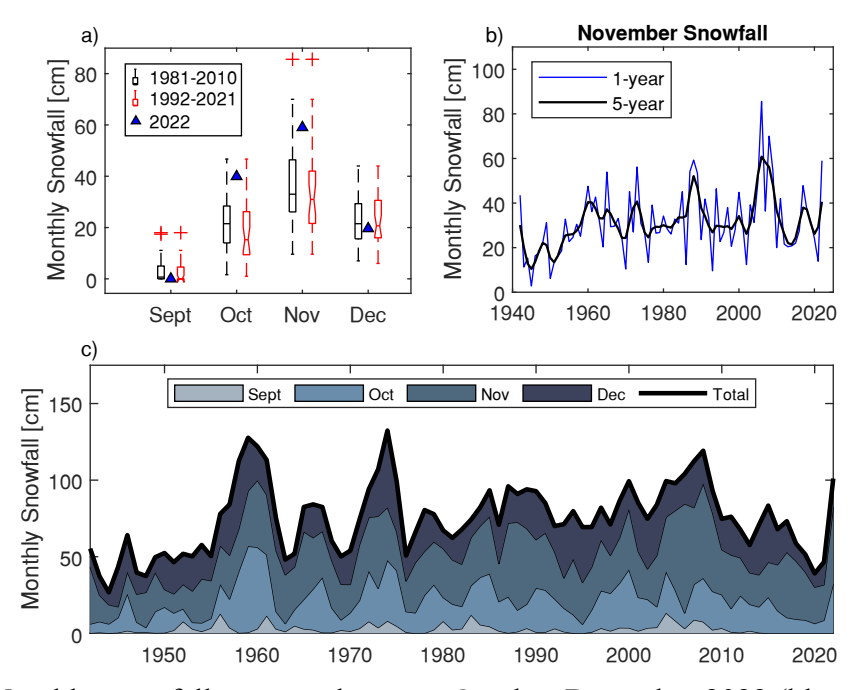


Figure 3. a) Monthly snowfall amounts between October-December 2022 (blue triangle) relative the 1981-2010 climate normal (black boxplot) and the preceding 30-year record (1992-2021; red boxplot). b) Long-term increasing trend in November snowfall recorded at the Yellowknife Airport Meteorological Station. c) Time series of snowfall from 1942-2022 highlighting the proportion of total snowfall (black line) between September - December.

3.2. Evolution of ice cover

3.2.1. Freeze-onset: skim ice production and melt

Landing Lake remained largely unfrozen between October 5th to 22nd, 2022. During this time, the lake was fully mixed. The initial occurrence of ice formation (freeze-onset) was on October 12th, 2022, where a brief period of skim ice was measured on the surface of the lake. Subsequently, three additional skim ice events were observed at the location of the floating research station, with durations ranging from 0.5-5.0 hours (Table 1; Figure 4). The formation of skim ice was initiated by rapidly declining air temperatures below the freezing point (Figure 4).

Lake surface temperatures cooled out of phase from the air temperature signal, as expected. The observed phase lags between variability in the air temperature and that of the surface waters typically ranged from 30 minutes to a couple of hours, depending on the initial temperature of the water.

Table 1. Timing of rapid formation and melt of skim ice on Landing Lake after freeze-onset and before ice-on.

Event	Skim Ice Formation	Skim Ice Melt	Duration	
	(MST)	(MST)	(Hr)	
1	Oct.12, 2022 22:30	Oct.13, 2022 03:30	5.0	
2	Oct.16, 2022 02:45	Oct.16, 2022 03:15	0.5	
3	Oct.18, 2022 02:15	Oct.18, 2022 05:15	3.0	
4	Oct.18, 2022 17:30	Oct.18, 2022 22:00	4.5	

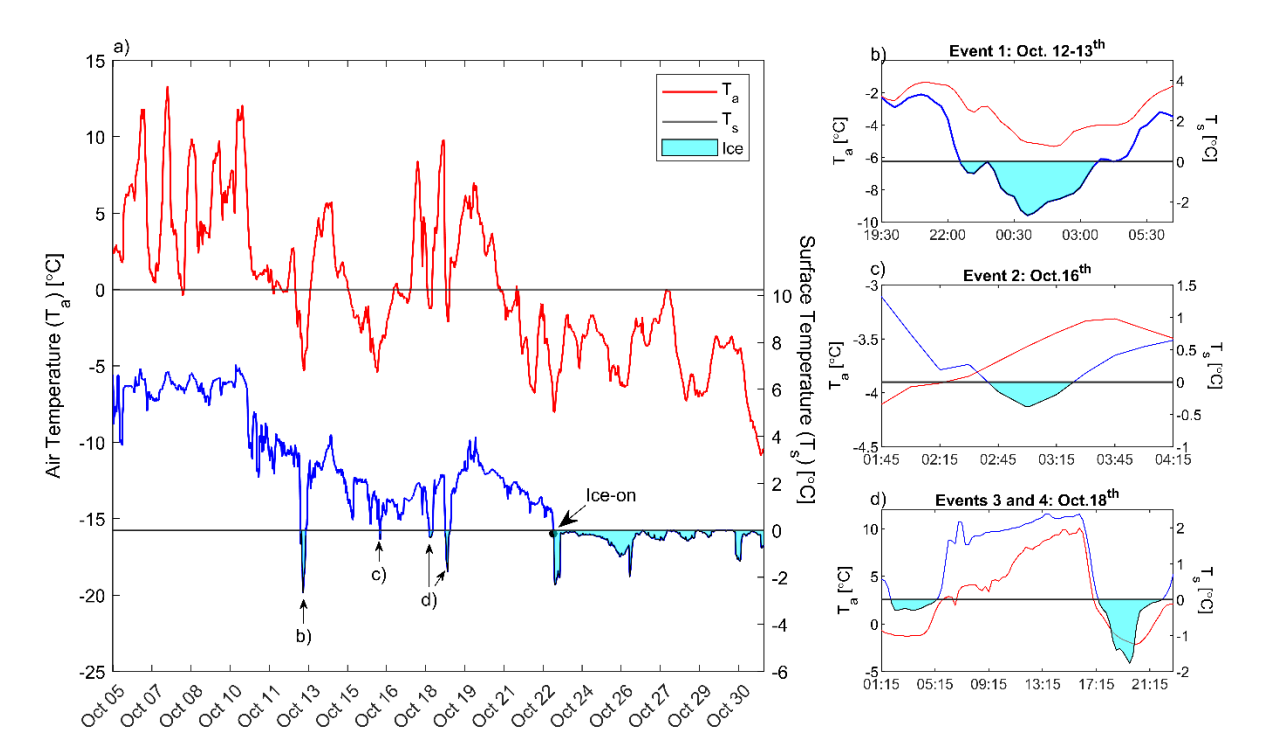


Figure 4. Rapid formation and melt of primary skim ice on Landing Lake prior to ice-on at October 23rd at 01:00. a) Lake surface temperatures (blue line) and air temperatures (red line) recorded by the SIMBA between October 5th-31st. The presence of skim ice is denoted by the light blue shading beneath the 0°C horizontal line. Note, the volume of light blue shading does not indicate the thickness of the skim ice. Figures b), c) and d) provide an enhanced view of the timing of the skim ice events. All times are presented in MST.

In Event 1 (Table 1), the formation of ice was directly driven by rapid surface cooling in response to two distinct periods of rapidly declining air temperatures. Between October 10th 14:30 and October 11th 01:15 (10.75 hours), air temperatures fell 11.4°C, resulting in a 1.8°C drop in the surface waters of Landing Lake (top 2 cm) (Figure 4). This temperature drop was equivalent to

141 J m⁻² of energy transferred to the atmosphere, or roughly 3.9 kW over the lake. Skim ice initiation was brought on by the subsequent fall in air temperatures from 2.3° C to -5.3° C between October 12^{th} 15:45 and October 13^{th} 02:00.

Event 2 was extremely short lived, with skim ice being present for only 30 minutes during the overnight periods when air temperatures fell below freezing to a low of -5.4°C. A phase lag of 30 minutes between the decline in air and surface water temperatures signals was identified. However, minimum water surface temperatures were reached 1.5 hours out of phase from minimum air temperatures. This increase in phase lag was likely attributed in part to a small latency effect from the formation (and melt) of the skim ice. Air and surface water temperatures quickly resynchronized as air temperatures continually warmed above the freezing point.

Events 3 and 4 occurred within 12.25 hours of one another. Lake water surface (and bulk; not shown) temperatures were cold (<2.3°C) and hence more sensitive to skim ice onset. As a result, skim ice was formed nearly in tandem with the onset of below freezing air temperatures. Notable fluctuations in air temperatures above and below 0°C drove the brief ice-free period between Events 3 and 4.

3.2.2. Freeze-up, slush, and snow-ice production

A stable ice cover began to form on Landing Lake after October 22nd after 12:00 MST within the southern and southwestern arms of the lake (Sentinel 2A optical image; not shown). The ice front progressed northward towards the deeper, central basin of the lake, with ice forming at the floating research station at 01:00 MST on October 23rd (Figure 5). The primary ice layer consisted of extremely thin skim ice, comprised of ice needles and dendrites (Figure 5b, c). The dendritic surface, rapid crystallization, and cool air temperatures (dropping to -8°C) on a calm water surface suggests the formation of P2 structured primary ice (Michel & Ramseier, 1971). The ice cover remained stable for a period of 17 hours. At 16:00, snowfall begin to fall and accumulate on the lake. By 18:00, the weight of accumulated snow became sufficient to induce cracking of the thin ice near the shoreline (Figure 5d).



Figure 5. The freeze-up of Landing Lake- south facing from the northern shore of the lake. The images show a) open-water, b) border ice, progressing from the southern, shallower portions of the lake, c) a solid, stable cover of skim ice, and d) the onset of slush formation along the shoreline due to increasing snow loads on the lake surface.

Between October 24th and November 4th, a considerable amount of snowfall, totaling 43.6 cm had fallen. The thickness of ice at the research station on October 23rd was only ~3 cm. As a result, the significant snowfall events (Figure 6) led to the production of substantial volumes of slush, which subsequently froze to produce snow-ice. Snow depths over the lake near the research station ranged between 3 and 20 cm as snow was consumed constructively for the growth of the snow-ice layer. The formation of snow-ice was evident through the upward movement of the ice surface position (Figure 6a), and through observing changes in ice thicknesses over time as shown in Figure 6b.

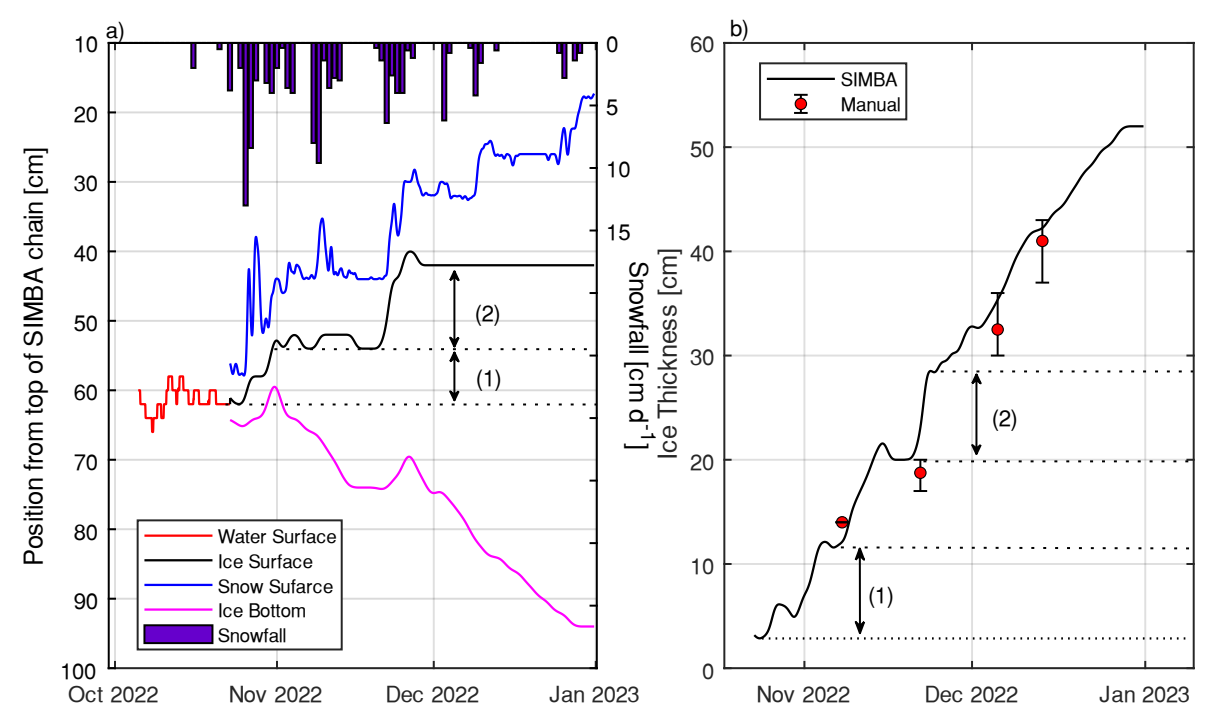


Figure 6. a) Interfaces between water, air, ice, and snow delineated using the SIMBA. Dotted lines and labels delineate periods where ice growth was primary driven by snow-ice production. b) Ice thicknesses between October 23rd and December 31st, 2022. Red circles represent the mean ice thickness surrounding the floating research station, measured through drilling boreholes in the ice. Error bars show the deviation in ice thicknesses at cardinal (N, S, W, E) directions around the station.

Field observations of near-shore (~5 m offshore) ice conditions on October 31st revealed complex ice stratigraphy, consisting of layers of snow-ice, unfrozen slush, and primary congelation ice (Figure 7). The total thickness of the near-shore ice was ~10 cm. The top of this layer was a 2.5 cm (1") layer of low-density frozen slush. The bottom layer of the ice was 2.5 cm (1") of congelation ice, while the middle ~5 cm (2") consisted of high-water content unfrozen slush. By November 30th, ice thicknesses had reached 32 cm, of which 20 cm was snow-ice. The remainder of the ice growth for the duration of the study period was exclusively from bottom ice growth, ranging between 0-1.3 cm d⁻¹.

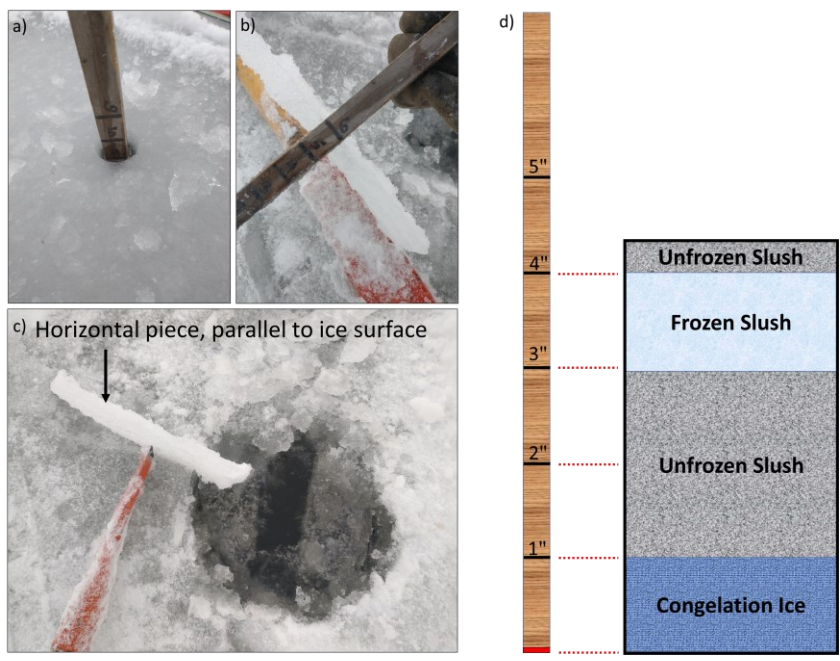


Figure 7. Stratigraphy of ice near the northern shore of Landing Lake observered on October 31st, 2022. a) Total thickness of ice (in inches) along a measuring rod. b) Photograph of frozen and unfrozen slush layers within the ice. c) Photograph of horizontal, low density, high porosity snow-ice (on chisel), and congelation ice (within within hole), and d) conceptual figure of the stratigraphy of the nearshore ice on October 31st, 2022.

3.2.3. Comparing lake ice evolution in 2021 and 2022

Ice thicknesses during the 2021-2022 ice cover season were previously monitored in Landing Lake between December 2021- March 2022 (Rafat et al., 2023). However, the device was not built on a raft and hence was deployed when the ice cover was 35 cm thick on December 6th, 2021. The evolution of the ice cover in December 2021 was very similar to December 2022 (Figure 8), despite significant differences in October and November snowfall between the years (Table 2). It should be noted that the SIMBA in 2021 was located ~500 m southwest of the location of the floating research raft presented in this study. However, the depth of the lake at both locations was nearly identical at ~3 m.

Although ice thicknesses in December were similar between the two years, the composition of and evolution of the ice prior to December were vastly different. This finding highlights the strong influence of early season ambient weather conditions on the evolution of ice cover in Landing Lake. In 2021, freeze-up was estimated to occur on November 4th, 2021 (Rafat et al., 2023) following a warm October (Table 2). The ice growth that followed was extremely rapid, reaching 19.4 cm by November 24th, and 35 cm by December 6th, 2021. In contrast, freeze-up in 2022 occurred nearly 2 weeks earlier, on October 23rd, 2022. The earlier freeze-up was however met with significant snowfall, which delayed and slowed the growth of congelation ice but contributed constructively to the formation of snow-ice. The two distinct paths in the growth of ice in October and November converged along a similar trajectory in December. Air temperatures in November and December were similar in 2021 and 2022. The later freeze-up in 2021 was attributed to significantly warmer October air temperatures in 2021 (Table 2). The ice cover in 2021 consisted

of almost exclusively of black ice, while that of 2022 was estimated to consist of up to \sim 63% snow-ice by the end of November.

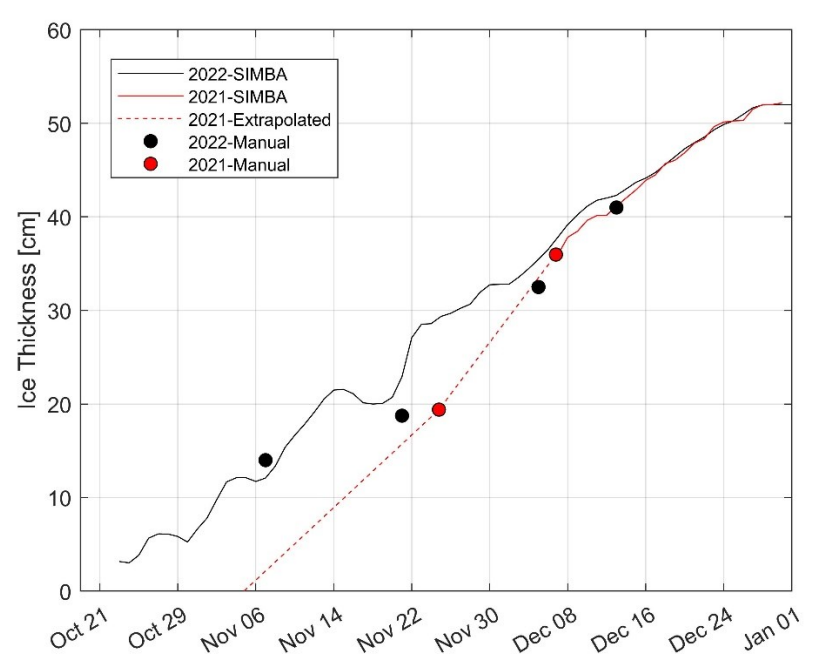


Figure 8. Comparison of the evolution of the ice cover in Landing Lake between 2021 and 2022. Circles represent borehole measurements taken from the ice cover at the floating research station in both 2021 and 2022.

Table 2. Comparison of air temperatures and snowfall between 2021, 2022, and the 1981-2010 climate normal

	Mean Daily Air Temperatures [°C]*			Monthly Snowfall [cm]*		
	Climate			Climate		
Month	Normal	2021	2022	Normal	2021	2022
	(1981-2010)			(1981-2010)		
September	7.2	8.7	9.7	3.5	0	0
October	-1.7	2.6	0.72	20.9	1	39.9
November	-13.7	-11.1	-11.8	36.5	13.9	59
December	-21.8	-27.7	-25.5	23.5	16	19.6

^{*}Measured at the Yellowknife Airport Meteorological Station

4. Discussion and Implications

Snowfall between 1942-2022 for October-December showed an increasing trend. This trend was largely a result of a statistically significant increasing trend in November snowfall in Yellowknife (Figure 3). This finding is complementary to those presented in Spence et al. (2011), which showed a decreasing monthly precipitation trend in October and increasing precipitation trend in September.

With the freeze-up of small lakes in Yellowknife typically occurring in late October/early November, increasing November snowfall has direct implications for the composition and

evolution of ice covers in the region. It is well known that in regions of significant snowfall, snow-ice may form a significant proportion of the total ice cover (e.g. Cheng et al., 2021). It is also understood that the bearing capacity of snow-ice is lower than congelation ice (Barrette, 2011; Masterson, 2009). Therefore, with increasing November snowfall, it may be reasonable to speculate that early season ice covers in Yellowknife may in the future consist of greater proportions of snow-ice as part of the total ice thickness. When ice covers are still thin, the formation of low density, high porosity snow-ice (Figure 7), combined with a reduced solid bottom fiber of congelation ice, may present a heightened risk of breakthrough accidents, through increasing the probability of breakthrough occurrences for a given date. However, during the spring melt, clear ice deteriorates faster than snow-ice due to its greater penetration depth and snow-ice's higher backscattering of solar radiation.

The evolution of the ice cover in December 2022 was shown to be peculiarly similar to that of December 2021 (Figure 8), despite significant differences in freeze-up dates, and snowfall between September-December (Table 2). This result suggests that despite a strong path dependency for the evolution of the ice cover in Landing Lake between the two years, the total thickness of the ice was nearly identical by the end of the study period. This result may be linked to similarities in air temperatures in November and December between the two years (Table 2) suggesting a strong air temperature dependence on ice growth (as expected). It is acknowledged however that ice growth is influenced by several competing environmental and meteorological conditions.

The presence of snow-ice in small lakes also influences lake thermal properties by significantly increasing the extinction coefficient (Bolsenga et al., 1996; Maguire, 1975) and surface albedo (Bolsenga, 1977) compared to clear congelation ice. The higher albedo delays break up processes (Leppäranta, 2015; Svacina et al., 2014), while the extinction coefficient controls the energy attenuation at the surface. These factors, in turn, impact convective mixing regimes within the lake during the ice cover season, particularly in the spring when the snow cover has melted.

5. Conclusion

This study investigated the formation and growth of the ice cover of Landing Lake, a small subarctic lake located ~12 km north of Yellowknife, Northwest Territories within the BCRW. Measurements of air, snow, ice, and water temperatures were collected at high spatial (2 cm) and temporal (15 minute) resolutions between October 5- December 31, 2022, which encompassed the open water, freeze-up, and early ice thickening periods in Landing Lake. This was achieved through designing and deploying a floating research station on the lake outfitted with an automated ice sensor called SIMBA. As a case study, the formation and growth of ice in October and November 2022 during a heavy snowfall year was contrasted with measurements obtained during a low snowfall year (October-December 2021).

Results from this study showed:

1) Total snowfall between 1942-2022 for the September-December period is increasing (p=0.02, α =0.05) at a rate of 0.32 cm y⁻¹, with an increasing trend in November snowfall (p=0.01, α =0.05) of 0.18 cm yr⁻¹.

- 2) The timing and magnitude of snowfall influenced the composition of the ice cover and its subsequent growth. Heavy snowfall occurring during and immediately following freeze-up induced significant snow-ice formation and reduced congelation ice growth.
- 3) The evolution of ice in December 2022 in Landing Lake was very similar to that of December 2021, despite significant differences in snowfall and freeze-up dates between the years.

Results presented have implications for ice safety and the usage of ice covers as transportation infrastructure. Should an increasing trend in November snowfall in Yellowknife continue, a shift in the composition of early season covers may follow suite. As snow-ice has lower bearing capacity than congelation ice, an additional design constraint and consideration may be necessary for the safe use of ice covers in the early season under a continual changing climate.

Acknowledgments

This research is funded and supported by Government of Northwest Territories, Environment and Climate Change, Cumulative Impact Monitoring Program (CIMP-212), the Natural Sciences and Engineering Research Council of Canada (NSERC), and Polar Knowledge Canada's Northern Scientific Training Program.

References

- Barrette, P. D. (2011). A laboratory study on the flexural strength of white ice and clear ice from the Rideau Canal skateway. *Canadian Journal of Civil Engineering*, 38(12). doi.org/10.1139/l11-106
- Bolsenga, S. J. (1977). Preliminary Observations on the Daily Variation of Ice Albedo. *Journal of Glaciology*, 18(80), 517–521. doi.org/10.3189/S0022143000021171
- Bolsenga, S. J., Evans, M., Vanderploeg, H. A., & Norton, D. G. (1996). PAR transmittance through thick, clear freshwater ice. *Hydrobiologia*, *330*, 227-230. doi.org/10.1007/BF00024210
- Cheng, B., Cheng, Y., Vihma, T., Kontu, A., Zheng, F., Lemmetyinen, J., Qiu, Y., & Pulliainen, J. (2021). Inter-annual variation in lake ice composition in the European Arctic: observations based on high-resolution thermistor strings. *Earth System Science Data*, *13*(8), 3967–3978. doi.org/10.5194/essd-13-3967-2021
- Duguay, C. R., Flato, G. M., Jeffries, M. O., Ménard, P., Morris, K., & Rouse, W. R. (2003). Ice-cover variability on shallow lakes at high latitudes: model simulations and observations. *Hydrological Processes*, 17(17), 3465–3483. doi.org/10.1002/hyp.1394
- Healy, J. J., de Groot, J. J., & Kestin, J. (1976). The theory of the transient hot-wire method for measuring thermal conductivity. *Physica B+C*, 82(2), 392–408. doi.org/10.1016/0378-4363(76)90203-5
- Jackson, K., Wilkinson, J., Maksym, T., Meldrum, D., Beckers, J., Haas, C., & Mackenzie, D. (2013). A novel and low-cost sea ice mass balance buoy. *Journal of Atmospheric and Oceanic Technology*, 30(11), 2676–2688. doi.org/10.1175/JTECH-D-13-00058.1
- Kheyrollah Pour, H., Duguay, C. R., Martynov, A., & Brown, L. C. (2012). Simulation of surface temperature and ice cover of large northern lakes with 1-D models: A comparison with MODIS satellite data and in situ measurements. *Tellus, Series A: Dynamic Meteorology and Oceanography*, 64(1). doi.org/10.3402/tellusa.v64i0.17614

- Kheyrollah Pour, H., Duguay, C. R., Scott, K. A., & Kang, K. K. (2017). Improvement of Lake Ice Thickness Retrieval from MODIS Satellite Data Using a Thermodynamic Model. *IEEE Transactions on Geoscience and Remote Sensing*, 55(10), 5956–5965. doi.org/10.1109/TGRS.2017.2718533
- Koo, Y., Lei, R., Cheng, Y., Cheng, B., Xie, H., Hoppmann, M., Kurtz, N. T., Ackley, S. F., & Mestas-Nuñez, A. M. (2021). Estimation of thermodynamic and dynamic contributions to sea ice growth in the Central Arctic using ICESat-2 and MOSAiC SIMBA buoy data. *Remote Sensing of Environment*, 267, 112730. doi.org/10.1016/j.rse.2021.112730
- Launiainen, J., & Cheng, B. (1998). Modelling of ice thermodynamics in natural water bodies. *Cold Regions Science and Technology*, 27(3), 153–178. doi.org/10.1016/S0165-232X(98)00009-3
- Lei, R., Cheng, B., Heil, P., Vihma, T., Wang, J., Ji, Q., & Zhang, Z. (2018). Seasonal and Interannual Variations of Sea Ice Mass Balance From the Central Arctic to the Greenland Sea. *Journal of Geophysical Research: Oceans*, 123(4), 2422–2439. doi.org/10.1002/2017JC013548
- Leppäranta, M. (2015). Freezing of Lakes and the Evolution of their Ice Cover. Springer Berlin Heidelberg. doi.org/10.1007/978-3-642-29081-7
- Lynch, M., Briggs, R., English, J., Khan, A. A., Khan, H., & Puestow, T. (2021). Operational Monitoring of River Ice on the Churchill River, Labrador. Proc. 21th Workshop on the Hydraulics of Ice Covered Rivers
- MacKay, M. D. (2012). A process-oriented small lake scheme for coupled climate modeling applications. *Journal of Hydrometeorology*, *13*(6), 1911–1924. doi.org/10.1175/JHM-D-11-0116.1
- Maguire, R. J. (1975). Light Transmission Through Snow and Ice. *Technical bulletin Inland Waters Directorate*; no. 91. Environment Canada
- Masterson, D. M. (2009). State of the art of ice bearing capacity and ice construction. *Cold Regions Science and Technology*, 58(3), 99–112. doi.org/10.1016/J.COLDREGIONS.2009.04.002
- Michel, B., & Ramseier, R. O. (1971). Classification of river and lake ice. *Canadian Geotechnical Journal*, 8(1), 36–45. doi.org/10.1139/t71-004
- Morse, P. D., & Wolfe, S. A. (2017). Long-Term River Icing Dynamics in Discontinuous Permafrost, Subarctic Canadian Shield. *Permafrost and Periglacial Processes*, 28(3), 580–586. doi.org/10.1002/ppp.1907
- Phillips, R. W., Spence, C., & Pomeroy, J. W. (2011). Connectivity and runoff dynamics in heterogeneous basins. *Hydrological Processes*, 25(19), 3061–3075. doi.org/10.1002/HYP.8123
- Rafat, A., Kheyrollah Pour, H., Spence, C., Palmer, M. J., & MacLean, A. (2023). An analysis of ice growth and temperature dynamics in two Canadian subarctic lakes. *Cold Regions Science and Technology*, 210, 103808. doi.org/10.1016/j.coldregions.2023.103808
- Spence, C., Guan, X. J., Phillips, R., Hedstrom, N., Granger, R., & Reid, B. (2010). Storage dynamics and streamflow in a catchment with a variable contributing area. *Hydrological Processes*, 24(16), 2209–2221. doi.org/10.1002/HYP.7492
- Spence, C., & Hedstrom, N. (2018). Hydrometeorological data from Baker Creek Research Watershed, Northwest Territories, Canada. *Earth System Science Data*, 10(4), 1753–1767.

- doi.org/10.5194/essd-10-1753-2018
- Spence, C., Kokelj, S. V, & Ehsanzadeh, E. (2011). Precipitation trends contribute to streamflow regime shifts in northern Canada. Proc. of symposium H02 held during IUGG2011 in Melborne Austraila.
- Svacina, N. A., Duguay, C. R., & King, J. M. L. (2014). Modelled and satellite-derived surface albedo of lake ice part II: Evaluation of MODIS albedo products. *Hydrological Processes*, 28(16), 4562–4572. doi.org/10.1002/hyp.10257
- Yang, Y., Leppäranta, M., Cheng, B., & Li, Z. (2012). Numerical modelling of snow and ice thicknesses in Lake Vanajavesi, Finland. *Tellus, Series A: Dynamic Meteorology and Oceanography*, 64(1). doi.org/10.3402/tellusa.v64i0.17202